

Leah Edelstein-Keshet · G. Bard Ermentrout

A model for actin-filament length distribution in a lamellipod

Received: 19 May 2000 / Revised version: 12 March 2001 /
Published online: 19 September 2001 – © Springer-Verlag 2001

Abstract. A mathematical model is derived to describe the distributions of lengths of cytoskeletal actin filaments, along a 1 D transect of the lamellipod (or along the axis of a filopod) in an animal cell. We use the facts that actin filament barbed ends are aligned towards the cell membrane and that these ends grow rapidly in the presence of actin monomer as long as they are uncapped. Once a barbed end is capped, its filament tends to be degraded by fragmentation or depolymerization. Both the growth (by polymerization) and the fragmentation by actin-cutting agents are depicted in the model, which takes into account the dependence of cutting probability on the position along a filament. It is assumed that barbed ends are capped rapidly away from the cell membrane. The model consists of a system of discrete-integro-PDE's that describe the densities of barbed filament ends as a function of spatial position and length of their actin filament "tails". The population of capped barbed ends and their trailing filaments is similarly represented. This formulation allows us to investigate hypotheses about the fragmentation and polymerization of filaments in a caricature of the lamellipod and compare theoretical and observed actin density profiles.

1. Introduction

The shape of an animal cell, its motility, and many of its functional properties are controlled by the cytoskeleton, whose major components include microtubules, intermediate filaments, and actin. Actin is by far the most abundant protein, and its dynamics have been under intense experimental and theoretical scrutiny. Details about the polymerization and depolymerization, capping and uncapping, and regulation of actin dynamics have emerged from experimental and theoretical studies. Polymerized actin forms filaments (F-actin) with distinct ends. The "barbed" (or plus) end is the preferred nucleation site for monomers, whereas the "pointed" (or minus) end generally depolymerizes under conditions in the cell. New actin-binding proteins that have one effect or another are discovered continually. Some of these regulate actin at the monomer level (profilin), some alter or influence actin polymerization kinetics (ADF/cofilin, profilin), others chop, fragment or

L. Edelstein-Keshet (to whom reprint requests should be addressed): Department of Mathematics, University of British Columbia, Vancouver, BC, Canada, V6T 1Z2. e-mail: keshet@math.ubc.ca

G.B. Ermentrout: Department of Mathematics, University of Pittsburgh, Pittsburgh, PA 15260, USA. e-mail: bard@math.pitt.edu

Key words or phrases: Actin filament dynamics – Actin-length distribution – Polymerization – Fragmentation – Mathematical modelling – Integro-partial differential equations

degrade actin filaments (gelsolin, cofilin), while still others bind filaments together into a network (alpha-actinin, filamin) or promote nucleation and side-branching (Arp2/3). Mechanisms that regulate these events are still not well understood (Bailly et al., 1999). Further, how the details of the picture fit together into a coordinated whole is still unclear.

One of the controversies surrounding actin dynamics is how the filaments and their tips are distributed in the lamellipodium. Many biologists believe that actin filament barbed ends are associated with the membrane of the cell (Small et al., 1995a). However, whether the filaments are of uniform length, or whether there is a distribution of pointed ends and barbed ends throughout the lamellipod is an outstanding question (Heath and Holifield, 1991). The difficulty of this question resides in the fact that it is currently impossible to quantify and identify all the filament ends (Ryder et al., 1984). A further important issue is whether actin filaments are actively cut as part of the natural turnover in the lamellipod, and if so, how this process affects filament distribution. Proteins that cut or promote disassembly of actin, notably gelsolin and ADF/cofilin are well known, but their precise action and importance *in vivo* is controversial. Such questions are closely linked to the fundamental issue of how actin dynamics is linked to cell motility. Since the ends of the filaments are the only sites for elongation, and, in particular, the barbed ends are favored for adding monomers, the distribution of filament lengths – and hence of their ends – is important for determining the way that polymerization and growth is distributed in the lamellipodium. The abundance of such intriguing questions suggests that a framework for testing hypotheses about spatial dynamics could be a useful additional tool in research on actin.

In this paper, we will use mathematical modelling to explore hypotheses about the behaviour of cytoskeletal remodelling in the leading edge of an animal cell, the lamellipodium. We are specifically interested in how the various possible interactions - including polymerization, fragmentation, capping, etc, can shape the spatial and length distribution of the actin filaments. Recent models for actin polymerization and fragmentation dynamics include previous papers by the authors (1998; 1998). However, the treatment of the process as *spatially distributed* is new to this paper. In this first step, we will restrict attention to a simplified geometry. We assume that actin filaments are polarized with their axis essentially perpendicular to, and with their barbed ends directed towards the leading edge of the cell. This allows one to replace a three-dimensional problem with a single space dimension. The fact that the lamellipodium is quite thin, about 180 nm, see (Bailly et al., 1999), compared with its length, which is up to 10 μ , suggests that this is a reasonable first approximation to a more detailed treatment.

2. Biological background

2.1. Typical sizes and time scales involved

The width of lamellipodia vary in cells, from under one micron, to around 10 microns. For example, polymorphonuclear leukocytes (PMN) have lamellipodia roughly 0.2 μ in diameter (Zigmond, 1993). Rates of motion also vary greatly.

PMN's can exhibit forward protrusion as rapid as $30\mu/\text{min}$ (Zigmond, 1993). Other typical rates of protrusion include $2.4\mu/\text{min}$ in fish keratocytes, and as low as $0.4\mu/\text{min}$, $0.08\mu/\text{min}$ in (respectively) human and mouse fibroblasts (Theriot, 1994). The half-life of F-actin in cells has been observed to be 3 sec in PMN (Zigmond, 1993), 23 sec in keratocytes, 33 sec in the actin "comet tail" of the parasite *Lysteria monocytogenes*, 55 sec in the human fibroblasts, and 181 sec in mouse fibroblasts (Theriot, 1994). The mean length of actin filaments in various types of cells also varies: for example, $0.2\mu\text{m}$ in PMN, $0.6\mu\text{m}$ in macrophages, and $0.1\text{--}0.3\mu\text{m}$ in platelets (Zigmond, 1993). Some sketches and comparisons of typical actin filament density distributions across structures such as the lamellipodia in keratocytes, fibroblasts, and across the *Lysteria* comet tail are shown in (Theriot, 1994). Differences include the sharpness of the rise of density close to the leading edge, the plateau-like density in the intermediate zone (keratocyte), the gradual drop (fibroblast) or the exponential decay with distance in the back (*Lysteria*).

2.2. Length and distribution of filaments and their ends

Experimental data on filament length distributions *in vivo* comes from a variety of direct and indirect observations. Direct visualization involves microscopy. Such observations of fish keratocytes have demonstrated that long filaments span the entire lamellipod (Small et al., 1995a). An indirect method involves analysis of the time course of depolymerization under various conditions. For example, length distributions of actin filaments in PMN's was ascertained by following depolymerization from pointed ends for filaments whose barbed ends were blocked by cytochalasin (Cassimeris et al., 1990; Cano et al., 1991; Redmond and Zigmond, 1993; Cano et al., 1992). They found that most filaments are shorter than 0.18μ , with a smaller fraction in the range $0.18 - 1\mu$.

Fluorescence photoactivation experiments reveal a roughly uniform rate of turnover across the lamellipodium, difficult to reconcile with pointed ends concentrated at one place (Theriot and Mitchison, 1991). Similar studies have been used (Theriot, 1994) to argue that the gradient of filamentous actin observed across the lamellipodia of many cell types is too shallow, given kinetics of turnover of these structures, to be reconciled with polymerization occurring only at the membrane. This has led to the idea that the fast growing "barbed ends" must also be distributed throughout the structure. These ideas are still controversial.

Fluorescent markers such as rhodamine and phalloidin have been applied in preparations of polymorphonuclear leukocytes before and after stimulation by chemoattractants (Redmond and Zigmond, 1993). It was found that the distribution of actin polymerization (assumed to coincide with the distribution of free barbed ends) was similar to the distribution of F-actin throughout the cell. One way of interpreting this is that the number of free barbed ends is therefore approximately constant along the length of the lamellipod, and that the mean filament length is also roughly the same across this structure. Another interpretation would be that filaments are rapidly cut, producing new barbed ends that would polymerize freely.

These findings are in contrast with results of Bailly et al (1999) in which nucleation sites (filament ends) in moving cells were shown to be concentrated at the

leading edge of mammary carcinoma cells. The authors stimulated cells with epidermal growth factor (EGF), permeabilized the cells, and tagged nucleation sites with rhodamine-actin. Figure 6 of their paper shows a distinct peak of nucleation sites close to the membrane, and a graded filament density that falls off with a much gentler slope towards the rear. More quantitative results about actin density distributions are cited and described in the discussion section of this paper.

2.3. Regulation of growth and polymerization of actin

The regulation of actin polymerization occurs at a number of levels, briefly reviewed below.

Monomer availability. An important role is played by actin-associated proteins, such as profilin and thymosin, in sequestering free monomers and regulating their ability to polymerize. The concentration of actin subunits in the cell exceeds $100\mu M$, far in excess of the level at which normal polymerization rates occur, so that polymerization is essentially free of diffusional limitations. A detailed treatment of the spatially distributed monomer cycle has been carried out by (Mogilner and Edelstein-Keshet, 2001).

Barbed end capping. Under normal conditions, most actin filament barbed ends not in proximity to the membrane are capped (Coluccio and Tilney, 1983; Schafer et al., 1996; Janmey, 1994; Theriot, 1994). Most capping proteins require high calcium levels, and are inhibited by membrane-associated phosphoinositides. Caps are released when the cell is stimulated by signals such as chemoattractants or growth factors (Zigmond, 1993; Redmond and Zigmond, 1993; Schafer et al., 1996; Isenberg and Niggli, 1998).

Filament cutting. A variety of proteins cut or fragment actin filaments. These include gelsolin, a strong fragmenter which also acts as a capper and a nucleation site (Howard et al., 1990; Lind et al., 1987). Gelsolin caps have a half life of 30 minutes, much longer than the time scale of other cytoskeletal dynamics. A second group of actin cutters includes the ADF/Cofilin family. These fragmenters do not attach to the severed ends of the filament, but they may also be involved in accelerating the depolymerization of actin monomers at the pointed ends of filaments (Moon and Drubin, 1995; Meberg et al., 1998; Carlier et al., 1997). Details of the interactions of actin cutters with membrane lipids such as phosphoinositides and calcium is reviewed in recent papers (Janmey, 1994; Isenberg and Niggli, 1998).

The importance of actin fragmentation in cell motility is still controversial. For example, the level of gelsolin does not correlate strictly with motility and seems highly dependent on cell type and degree of differentiation of the cell; some mutants lacking gelsolin can have normal cell motility (Witke et al., 1995). However, the fragmenting activity of gelsolin has been shown to correlate with fibroblast migration recently (Arora and McCulloch, 1996) and increasing the content of

gelsolin in mouse fibroblasts has been shown to increase the rate of migration of the cells (Cunningham et al., 1991). It was further shown (Arora and McCulloch, 1996) that the distribution of gelsolin in migrating cells is diffuse, i.e. not clustered at membranes or other structures. We will interpret this to mean that the distribution of cutting agents such as gelsolin or cofilin is fairly uniform inside the cell.

ATP hydrolysis and monomer activation. The monomers along an actin filament are not all the same. The newly polymerized monomers close to the barbed end are associated with Adenosine Tri-Phosphate (ATP) nucleotides. The ATP is cleaved at a rate of 13 sec^{-1} to $ADP - P_i$. This means that only about one actin subunit at the barbed end of a filament is in the ATP bound form (Dufort and Lumsden, 1996). Further into the filament, the $ADP - P_i$ is also broken down: the P_i is released slowly with a first-order kinetics and a rate constant of about 0.006 sec^{-1} (Korn et al., 1987) so that the monomers are gradually converted to ADP-associated actin. An excellent review of the nucleotide processing and regulation of actin is given by Paul Dufort in his recent PhD thesis (Dufort, 2000). A regulatory role of the nucleotide composition of filaments has been proposed (Carrier and Pantaloni, 1997; Dufort and Lumsden, 1996). It is known that molecules that cut actin filaments, including gelsolin and the ADF/cofilin family preferentially act on ADP actin monomer portions of the filament. If we assume that polymerization to ATP-actin is most prevalent near the membrane, and that a filament loses monomers from its non-membrane pointed end (i.e. that the filament as a whole is treadmilling) it is reasonable to suppose that the probability of cutting increases along the length of the filament from its barbed end. This type of assumption will be incorporated into our model. We note, however, that there is some controversy still about whether filaments do treadmill *in vivo* – see, for example (Dufort, 2000).

3. Development of the Model

3.1. Motivation

In a set of previous papers we discussed the length distribution of actin filaments which were polymerizing and depolymerizing, and which were being fragmented by an agent such as gelsolin (Edelstein-Keshet and Ermentrout, 1998; Ermentrout and Edelstein-Keshet, 1998). Our goal now is to explicitly consider how these processes are organized with respect to the spatial distribution of the filaments in a model lamellipod. We first derive equations to keep track of spatial (and length) distributions, and then use these equations to examine a steady state situation. Our purpose here is not to consider the details of protrusion velocity and how the actin polymerization mechanism translates into motion of the cell. Such mechanochemical details are under separate investigation (Mogilner and Edelstein-Keshet, 2001). Here we are interested only in the lengths and spatial distributions of the cytoskeletal actin filaments, and how capping and cutting affects the actin density distribution in the lamellipod.

3.2. Definitions and notation

$a(x, t)$	Concentration of actin monomers at position x and time t
$b_a(x, l, t)$	Density of active barbed ends at position x with filament of length l attached to them
$b_c(x, l, t)$	Density of capped barbed ends at position x with filament of length l attached to them
k_b^+	Polymerization rate constant for fast growing “barbed” end of filament
k_b^-	Depolymerization rate for fast growing “barbed” end of filament
k_p^+	Polymerization rate constant for slow growing “pointed” end of filament
k_p^-	Depolymerization rate for slow growing “pointed” end of filament
$v_b(t) = (k_b^+ a - k_b^-)$	Apparent rate of motion of the barbed end of a filament
$v_p(t) = (k_p^+ a - k_p^-)$	Apparent rate of motion of the pointed end of a filament
δ	Length change associated with polymerization of a single monomer
g	Concentration of actin filament chopper
$P(l)$	Filament cutting probability at distance l from an active barbed end

3.3. Derivation of the equations

We will consider uncapped barbed ends which can polymerize monomer, henceforth called **active barbed ends**, and those that are capped and stationary, as well as pointed ends. In view of the biological background, we can assume that a capped barbed end is essentially stable on the time scale of the other processes, unless it is in proximity to the membrane. We will further assume that most of the active barbed ends of filaments are located in close proximity to the cell membrane.

It will be assumed that conditions are such that active barbed ends grow by polymerization and pointed ends lose monomers via depolymerization. (We do not specify the exact conditions, which may consist of monomer distribution, presence of actin-associated proteins such as depolymerization factors, etc.) The velocity of motion of the barbed and pointed ends will be taken as v_b and v_p respectively (except for capped barbed ends, which do not move).

An agent that chops filaments and caps their barbed ends (similar, but not necessarily restricted to the protein gelsolin) will be modelled, and we investigate how it affects the length distribution of the actin filaments in space. To develop the model we consider all possible transitions that can take place when filaments lengthen, shorten, or are cut.

1 Geometry. We simplify to a one dimensional setting, as would occur in a filopod or in a lamellipod in which the filaments are highly polarized, with barbed ends pointing towards the membrane (which coincides with the direction of growth).

Assuming a one dimensional geometry is a simplification for mathematical tractability at this preliminary modelling stage. It is suitable for describing filopodia, but may not be as accurate for a lamellipod where the filaments have more variance in their orientation.

- 2 Behaviour at the membrane.** We assume that there is a pool of actively growing barbed ends at, or close to this site. This assumption fits well with current biological views. (After transforming our model equations to a moving coordinate system, the membrane will be located at $x = 0$.)
- 3 Motion of ends.** An active barbed end can add one monomer during a small time interval Δt , leading to displacement of the tip forward and lengthening of the filament by an amount δ . We assume that the pointed end of the actin filament can only *lose monomers* under the conditions in the lamellipod. (See, in particular, the effect of ADF/cofilin discussed above.) This shortens the filament, displacing the pointed tip in the positive x direction by an amount δ . See Figure 1.
- 4 Filament motion.** We assume that a filament does not undergo significant translational diffusion motion as a whole. This is reasonable in view of the abundance of crosslinking proteins that would tend to keep most filaments tethered, but it, too, is an approximation.
- 5 Cutting.** In the absence of evidence to the contrary, we will assume that actin fragmenting agents are distributed uniformly in space. However, in keeping with remarks in the introduction, it will be assumed that the probability of fragmentation at some site along a given filament depends on distance away from the barbed end of the filament.

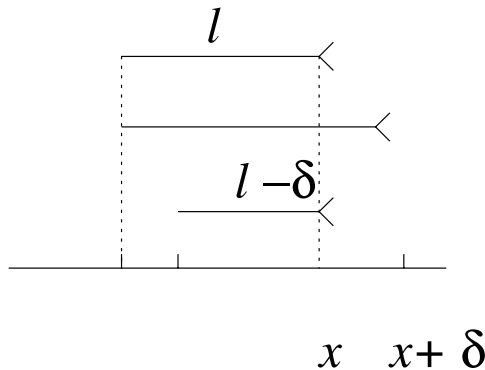


Fig. 1. Filaments with uncapped (“active”) barbed ends can undergo the polymerization-induced changes shown in this sketch. The position of the end can move forward due to monomer addition at the barbed end (represented by forked end). The length of the filament can shorten due to depolymerization at the pointed end. This will contribute to the change of density of filaments of length l at the position x , represented by the variable $b_a(x, l, t)$. Changes in length due to a monomer (size increment represented by δ) are exaggerated for the purposes of this sketch. The fork-like appendages at one end of the polymer are only meant to distinguish the fast growing “barbed ends” which all point towards the front from the opposite “pointed” ends. These polymers are not branched.

6 Capping. By capping we mean the inactivation of a barbed end of an actin filament so that it cannot polymerize monomers. Capped filaments cannot grow in length. However, they can shorten at their pointed ends and depolymerize completely. See Figure 2.

7 Cutting and capping. When appropriate, we will consider the distinction between fragmenters such as gelsolin that cut and cap the newly formed barbed end (see Figure 3), versus those, such as cofilin, that simply cut the filament.

The fact that cutting depends on position along a filament leads us to formulate our models in terms of the position of the barbed end of a filament, whether capped or uncapped, and the length of the filament trailing behind it. (The positions of the pointed ends of the filaments can easily be inferred from this as well, if desired, but will be irrelevant to considerations in this paper.)

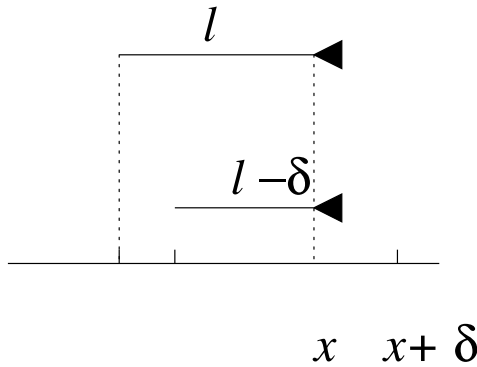


Fig. 2. Filaments with capped barbed ends can only lose monomer at their pointed (uncapped) ends. (Under the conditions described in this paper, it is assumed that these ends are all depolymerizing, causing shortening of these filaments.) The density of capped filaments at x with length l is represented by the variable $b_c(x, l, t)$.

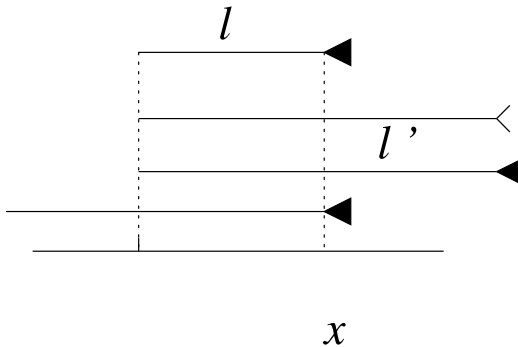


Fig. 3. A filament of length l with barbed end at x (top) can also be created by one of three ways by fragmentation of a longer uncapped or capped filament at the position x , or at the position $x - l$.

The transitions described above can be summarized as follows:

$$\begin{aligned}
 b_a(x, l, t) & \begin{cases} \rightarrow b_a(x + \delta, l + \delta, t + dt) & \text{polymerization of barbed end} \\ \rightarrow b_a(x, l - \delta, t + dt) & \text{depolymerization of pointed end} \end{cases} \\
 b_c(x, l, t) & \begin{cases} \rightarrow b_c(x, l - \delta, t + dt) & \text{depolymerization of pointed end} \\ \leftarrow b_a(x + l', l + l', t + dt) & \text{cut and cap active filament} \\ \leftarrow b_c(x + l', l + l', t + dt) & \text{cut and cap capped filament} \\ \leftarrow b_c(x, l + l', t + dt) & \text{cut and cap capped filament} \end{cases}
 \end{aligned}$$

We will occasionally refer to the “head” or “tail” of a filament, by which we mean the portion next to the barbed, respectively pointed, end. The transitions described above lead to the following equations written in terms of the barbed ends of filaments:

Case 1. Fragmentation without capping:

In this case, we need only consider an equation for the active barbed ends, which would be:

$$\begin{aligned}
 \frac{\partial b_a(x, l, t)}{\partial t} &= v_b[b_a(x - \delta, l - \delta, t) - b_a(x, l, t)] + v_p[b_a(x, l + \delta, t) - b_a(x, l, t)] \\
 &+ gP(l) \int_l^\infty b_a(x, s, t) ds \\
 &+ g \int_x^{x_{max}} b_a(y, y - x + l, t)P(y - x) dy \\
 &- gb_a(x, l, t) \int_0^l P(s) ds. \tag{1}
 \end{aligned}$$

The terms with coefficients v_p, v_b keep track of the transitions resulting from polymerization and/or depolymerization kinetics. These transitions include motion of the active barbed ends as well as elongation or shortening of their trailing filaments. The terms with the coefficient g result from fragmentation. The origin of our coordinate system is, so far, arbitrary. x_{max} represents the time-dependent position of the leading edge of the cell. The leading edge is not modelled explicitly, but we will assume that it moves in the positive direction with rate v_b , i.e at the speed of the actin filament polymerization. This is an approximation that neglects mechanical and thermodynamic considerations: a more careful treatment that shows how the velocity of protrusion of the leading edge depends on the number of active barbed ends at the membrane can be found elsewhere (Mogilner and Edelstein-Keshet, 2001). The individual terms above represent (a) polymerization and depolymerization that make longer (or shorter) filaments take on the length l , (b) chopping the tail off a longer filament so that its length becomes l , (c) chopping the head off a longer filament, or (d) eliminating an l length filament by cutting anywhere along its length.

Case 2. Cutting and capping:

In this case we must distinguish between filaments that were cut and capped and those that are still uncapped. A cutting event then always produces a capped filament, and we have the set of equations shown below:

$$\begin{aligned} \frac{\partial b_a(x, l, t)}{\partial t} = & v_b[b_a(x - \delta, l - \delta, t) - b_a(x, l, t)] + v_p[b_a(x, l + \delta, t) - b_a(x, l, t)] \\ & + gP(l) \int_l^\infty b_a(x, s, t) ds - gb_a(x, l, t) \int_0^l P(s) ds, \end{aligned} \quad (2)$$

$$\begin{aligned} \frac{\partial b_c(x, l, t)}{\partial t} = & v_p[b_c(x, l + \delta, t) - b_c(x, l, t)] \\ & + g \int_x^{x_{max}} b_a(y, y - x + l, t) P(y - x) dy \quad \text{Source term} \\ & + g \int_x^{x_{max}} b_c(y, y - x + l, t) P(y - x) dy \\ & + gP(l) \int_l^\infty b_c(x, l', t) dl' - gb_c(x, l, t) \int_0^l P(s) ds. \end{aligned} \quad (3)$$

In equation (3), the finite difference terms account for filament shortening due to depolymerization (at the pointed end of the filament), the ‘‘Source term’’ stems from cutting and capping of any filaments whose ends are active, and the other terms represent changes in the length distribution that result when filaments with capped barbed ends are chopped and capped yet again. The above equations have been formulated in a general coordinate system. The difference in the two versions of the model reflects the fact that cutting with capping converts an actively growing filament to a capped filament.

We observe that equation (2) for active tips is independent of equation (3), and can thus be treated separately. The only coupling occurs in the second term of equation (3). This term can be considered as a source term which is known once the solution for b_a is obtained from equation (2).

We can use the model above to predict the total density of filamentous actin as a function of position across the lamellipod. To do so, define

$$Z(x, t) = \int_{s=x}^{x_{max}} \int_{l=s-x}^\infty [b_a(s, l, t) + b_c(s, l, t)] dl ds \quad (4)$$

Then note that Z is a cumulative total contribution to density at x made by any filament long enough to reach x given that its (capped or uncapped) barbed end is at position s .

4. Analysis

4.1. Filaments with active barbed ends

In this section we will introduce further simplifying assumptions and explore their consequences. We focus attention on the cutting and capping equations, (2) and (3)

First, transform the equations to a coordinate frame moving with constant velocity, v_b . The leading edge will now be “frozen” at $x = 0$. Active barbed ends will be found close to $x = 0$, with their filaments trailing behind at negative values of x , inside the cell. (Recall that the compartment within 100–200 nm of the membrane provides a special environment in which uncapped barbed ends are favoured (Bailly et al., 1999)).

In moving coordinates, equation (2) is independent of x so that $b_a(x, l, t) = \Lambda(x)B_a(l, t)$ where $\Lambda(x)$ is the steady-state spatial density of active tips within the cell. We will discuss $\Lambda(x)$ subsequently. We can use equation (2), rewritten in terms of the $b_a(l, t)$, to characterize the length-dependent part of the distribution. We also approximate the finite difference terms by the first terms in a Taylor series expansion, obtaining:

$$\frac{\partial b_a(l, t)}{\partial t} = -\frac{\partial}{\partial l}b_a(v_b - v_p)\delta + gP(l) \int_l^\infty b_a(s, t) ds - gb_a(l, t) \int_0^l P(s) ds. \tag{5}$$

Define the new variables

$$z(l, t) = \int_l^\infty b_a(s, t) ds,$$

$$F(l) = \int_0^l P(s) ds.$$

$z(l)$ is the density of active filament ends whose filaments are longer than length l , and $F(l)$ is the cumulative probability that a filament will be broken at any position up to a distance l from its barbed end.

Suppose we assume that all the active barbed ends are at the membrane ($x = 0$), i.e. $\Lambda(x) = \delta(x)$. Then the quantity

$$z(x, t) = \int_{l=x}^\infty b_a(s, t) ds$$

can be interpreted as the density of actin filaments at position x and time t whose barbed ends are still uncapped.

Let $c = (v_b - v_p)\delta$. Then we can rewrite equation (5) as the system of two equations

$$\begin{aligned} \frac{\partial b_a(l, t)}{\partial t} &= -c \frac{\partial b_a}{\partial l} + gP(l)z - gF(l)b_a, \\ \frac{dz}{dl} &= -b_a. \end{aligned} \tag{6}$$

We look for a stationary solution $\partial b_a/\partial t = 0$, i.e we consider

$$\begin{aligned} 0 &= -c \frac{\partial b_a}{\partial l} + gP(l)z - gF(l)b_a, \\ \frac{dz}{dl} &= -b_a. \end{aligned} \tag{7}$$

Taking a second derivative of the z equation and using the first equation to eliminate $\partial b_a / \partial l$ leads to

$$\frac{d^2 z}{dl^2} = -\frac{\partial b_a}{\partial l} = -\frac{g}{c}(P(l)z - F(l)b_a).$$

Using the fact that $P(l) = dF/dl$ and $dz/dl = -b_a$, we can rewrite this as the second order equation

$$\frac{d^2 z}{dl^2} = -\frac{g}{c} \left(\frac{dF}{dl} z - F(l) \frac{dz}{dl} \right) = -\frac{g}{c} \frac{d}{dl} (Fz).$$

We can integrate once to obtain

$$\frac{dz}{dl} = -\frac{g}{c} (F(l)z) + K.$$

The constant of integration K in this equation is determined from the condition that there are no infinitely long filaments: $b_a \rightarrow 0$ and also $z \rightarrow 0$ as $l \rightarrow \infty$. This implies that $K = 0$. We can separate variables in the remaining equation and integrate once more to obtain

$$z(l) = Z_o \exp\left(-\frac{g}{c} \int_0^l F(s) ds\right).$$

We further find that

$$b_a(l) = -\frac{dz}{dl} = Z_o \frac{g}{c} F(l) \exp\left(-\frac{g}{c} \int_0^l F(s) ds\right). \quad (8)$$

The coefficient Z_o in equation (8) is given by

$$Z_o = z(0) = \int_0^\infty b_a(s, t) ds = B.$$

We now make a number of specific assumptions about the probability of cutting along the length of a filament and arrive at the detailed distribution of filament lengths that result in each case.

4.1.1. Example 1: Cutting equally probable everywhere

In this case, $P(l) = p = \text{constant}$, i.e. a filament has equal probability of being cut anywhere along its length. Then we find that

$$F(l) = \int_0^l P(x) dx = pl,$$

$$\int_0^l F(s) ds = p \frac{l^2}{2},$$

so that

$$b_a(l) = \hat{B} \frac{gp}{c} l \exp\left(-\frac{gp}{c} \frac{l^2}{2}\right).$$

The quantities \hat{B} and gp/c are just constants, and the shape of the distribution is as shown in the lower curve of Figure 4. This distribution would be obtained if the actin filaments are cut in a way **not** affected by the APT hydrolysis state of the monomers. i.e. where any site on the filament is equally likely to be cut.

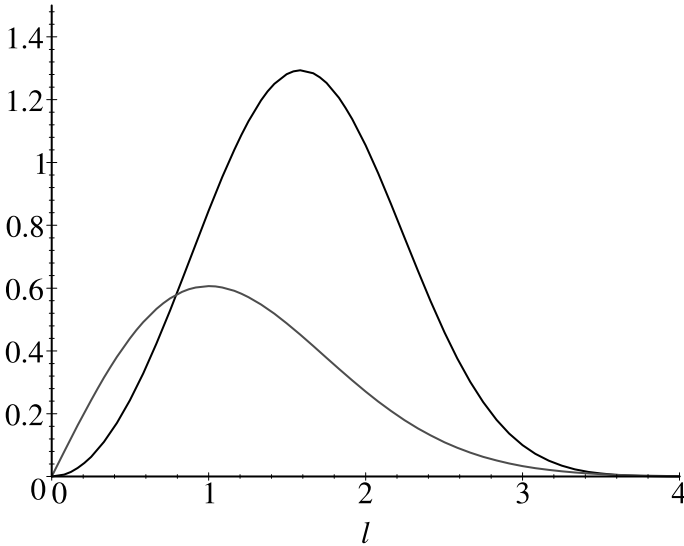


Fig. 4. The length distribution of filaments with active barbed ends is shown here for two cases:(1) the case that the probability of cutting is the same everywhere (lower curve). (2) the case that the probability of cutting decreases linearly along the length of the filament (higher curve). Horizontal axis: filament length. Vertical axis: stationary distribution for $b_a(l)$. Note that in case (1) there is a greater proportion of short filaments than in case (2).

4.1.2. *Example 2: Cutting probability increases linearly along filament*

In this case $P(l) = pl$. The calculations are similar to those done in the previous example, but the resulting distribution is

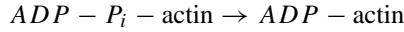
$$b_a(l) = B \frac{gp}{c} \frac{l^2}{2} \exp\left(-\frac{gp}{c} \frac{l^3}{6}\right).$$

This is also shown in Figure 4 (upper curve). The mean filament length is longer in this case, and the distribution is somewhat more symmetric about this mean.

4.1.3. *Example 3: A realistic cutting probability*

Following the literature on the ATP-hydrolysis cycle of actin, we can be more explicit about the actual probability of cutting along the length of a filament. As noted in the introduction, we assume that a transition takes place from *ATP*-actin to *ADP* - P_i and then to *ADP*-actin along the filament from its new to its older sites. This assumption would be consistent with the view that the filament is polymerizing mostly *ATP*-actin at the uncapped barbed ends close to the membrane, and depolymerizing “spent” actin (i.e. *ADP*-actin) at its pointed end. The idea is based on the view that, on average, treadmilling (i.e. the apparent movement of monomers down the length of a filament) is occurring. Note, however, that this assumption is still controversial, in view of (Dufort, 2000).

If we adopt the assumption that there is a transition from ATP to $ADP - P_i$ to ADP actin along the filament length, then we also find that the probability of cutting depends on position along the filament. The first transition is very rapid, with rate constant on the order of 13 sec^{-1} . The slower, rate limiting reaction is



with rate constant $k = 0.0055 \text{ sec}^{-1}$ (Carlier and Pantaloni, 1997; Dufort and Lumsden, 1996). The probability that a given monomer that starts out as $ADP - P_i$ at $t = 0$ is in the $ADP - P_i$ form at later time t satisfies the initial value problem

$$\frac{d[ADP - P_i]}{dt} = -k[ADP - P_i], \quad [ADP - P_i](0) = 1.$$

The solution is $[ADP - P_i](t) = \exp(-kt)$. The concentration of ADP -actin at the given position is then similarly $[ADP] = (1 - \exp(-kt))$. Taking into account the treadmilling of the filament (rate v) we can convert this time dependence to the probability that a monomer is in the ADP form when it has "travelled" a distance l down the filament. The result, which can be taken as the probability of cutting as a function of distance along the filament is:

$$P(l) = \left(1 - \exp\left(-\frac{k}{v}l\right)\right).$$

From the literature, we have $v \approx 5 \text{ sec}^{-1}$ as the cofilin stimulated treadmilling rate (Carlier et al., 1997), so that, combining this with the above value for k ,

$$P(l) = (1 - \exp(-rl))$$

where l is length in terms of monomer equivalents and $r = 0.0011$ per monomer. This cutting probability is shown in Figure 5.

Using this form of the cutting probability, we find that

$$F(l) = \int_0^l P(x)dx = l + \frac{1}{r}(e^{-rl} - 1),$$

$$\int_0^l F(s)ds = \frac{1}{2}l^2 - \frac{l}{r} + \frac{1}{r^2}(1 - e^{-rl}).$$

Setting $g/c = 1$ for convenience, we find that the shape of the distribution of filament lengths, $b_a(l)$ computed from equation (8) by forming

$$b_a(l) = F(l) \exp\left(-\int_0^l F(s)ds\right)$$

is as shown in Figure 6.

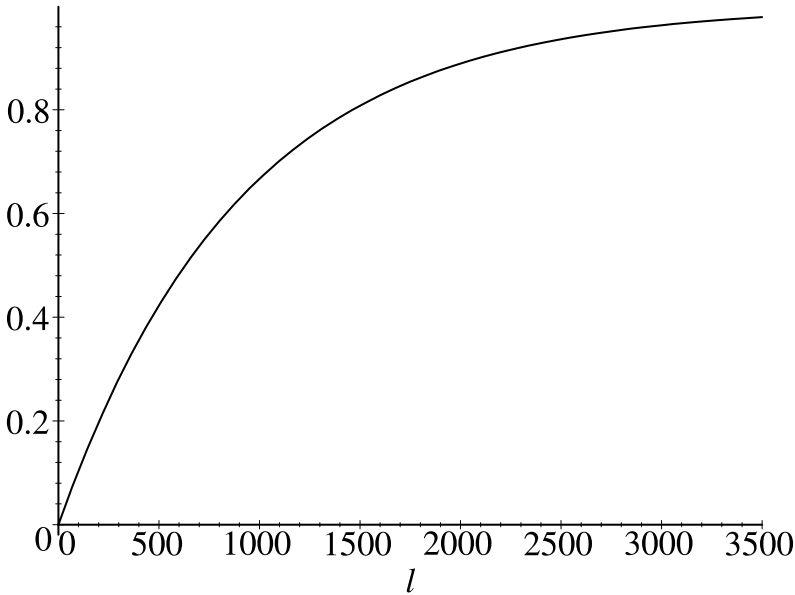


Fig. 5. The probability of finding an ADP-actin, and hence the probability that the filament will be severed by one of the cutting proteins, as a function of length (in monomer subunits) along the filament from the barbed end. The length shown corresponds roughly to a 10μ filament treadmilling at the accelerated rate of 5 subunits per second, as in the presence of ADF/cofilin.

4.2. Behaviour of the capped filaments

As discussed, according to our model, there is continual deposition of a “residue” of old filaments whose barbed ends are capped. These filaments are essentially immobile, but are continually being digested away by depolymerization from their pointed ends. In one sense, the population of capped filaments are uninteresting, as they are destined to be destroyed and recycled into new filaments (by processes not here made explicit; note that we have not discussed how actin monomers are recycled, and have taken the simple view that these monomers are plentiful everywhere.) From that perspective, modelling their behaviour is less interesting than that of the active filaments. Further, this modelling turns out to be more complex.

On the other hand, the capped filaments are still part of the overall actin filament density, and thus would show up in any experiment that determines the density of polymerized actin across a cell or lamellipod. We can say something about the nature of these residual filaments by investigating equation (3).

The use of moving coordinates did not affect the analysis of the active barbed end filaments: the barbed ends just move forward at velocity, v_b , and none are created *de novo*. This meant that we only needed to analyze the filament length distribution. However, for the capped filaments, which do not grow, we must include the spatial aspect of the problem. This is facilitated by replacing the space variable, x with the moving coordinate, $\xi = v_b t - x$ and setting $x_{max} = v_b t$ so that this

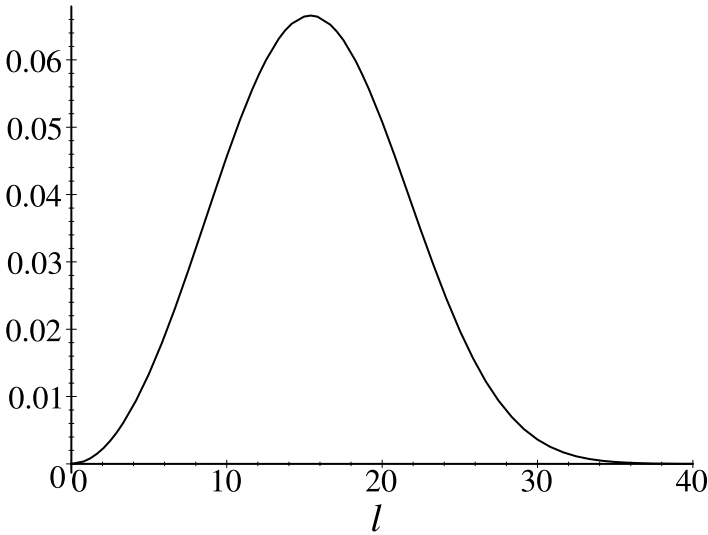


Fig. 6. The length distribution of filaments with active barbed ends is shown here for a more realistic cutting distribution, which uses the fact that cutting is most likely when the filaments are in the ADP-actin form. See text for details.

corresponds to $\xi = 0$. In these coordinates, the domain of integration $[x, x_{max}]$ becomes $[0, \xi]$ with positive values of ξ corresponding to values of x below x_{max} . Using a similar approximation for the polymerization terms, Equation (3) for the capped filament ends in (ξ, l, t) coordinates can be rewritten in the form

$$\begin{aligned}
 \frac{\partial b_c(x, l, t)}{\partial t} + v_b \frac{\partial b_c(x, l, t)}{\partial \xi} &= v_p \frac{\partial b_c(\xi, l, t)}{\partial l} \\
 &+ S(\xi, l) \quad \text{“Source term”} \\
 &+ g \int_0^\xi b_c(y, \xi - \eta + l, t) P(\xi - \eta) d\eta \\
 &+ g P(l) \int_l^\infty b_c(\xi, l', t) dl' \\
 &- g b_c(\xi, l, t) \int_0^l P(s) ds. \tag{9}
 \end{aligned}$$

The source term is found as follows, after transforming to moving coordinates:

$$S(\xi, l) = \int_x^{x_{max}} b_a(y, y-x+l, t) P(y-x) dy = \int_0^\xi \Lambda(\eta) B_a(\xi-\eta+l) P(\xi-\eta) d\eta$$

where $B_a(l)$ is the known stationary length distribution of the filaments trailing behind the active barbed ends. Here we have used the assumption that the active tips have a fixed density. In particular, we will consider only the case $\Lambda(\xi) = \delta(\xi)$,

i.e that the active barbed ends are concentrated at the edge, at $\xi = 0$. Then the only contribution to the “source” integral occurs at $\eta = 0$ so that

$$S(\xi, l) = P(\xi)B_a(l + \xi).$$

We will assume that the capped filaments are mostly in the ADP-actin form already, and so, are equally likely to be broken anywhere along their length. To explore the steady-state distribution of the capped filaments set $\partial b_c/\partial t = 0$. Let $B(\xi, l)$ denote this stationary density distribution. Then

$$\begin{aligned} v_b \frac{\partial B}{\partial \xi} &= v_p \frac{\partial B}{\partial \ell} + gP(\xi)B_a(\xi + \ell) \\ &+ g \int_0^\xi B(y, \xi - y + \ell)P(\xi - y) dy \\ &+ gP(\ell) \int_\ell^\infty B(\xi, \ell') d\ell' \\ &- gB(\xi, \ell) \int_0^\ell P(\ell') d\ell'. \end{aligned} \tag{10}$$

We impose the additional condition that there are *no* capped filaments at the membrane:

$$B(0, \ell) = 0.$$

In absence of the source term, B will tend to zero as eventually all capped filaments will be chopped up. For the moment, consider the case when no fragmentation occurs, $g = 0$. Then the equation simplifies to

$$v_b B_\xi - v_p B_\ell = 0.$$

The general solution to this is:

$$B(\xi, \ell) = Q(v_p \xi + v_b \ell).$$

The boundary condition is $B(0, \ell) = 0$ so $Q(v_b \ell) = 0$ which means that $Q \equiv 0$ so that in absence of choppers, there will be no capped filaments at all. This is intuitively clear: all the ends are concentrated at the membrane, where they are prevented from being capped, as discussed before. This holds as long as we neglect nucleation, as we have been doing in this paper. Thus, the source term is important in maintaining the pool of capped filaments.

Equation (10) is a linear PDE, but, due to its complicated form, is unlikely to admit a closed form solution. So, consider the following approximate solution. Using the fact that $B = 0$ when $g = 0$, we may suppose that $B = gb = g(b_0 + gb_1 + g^2b_2 + \dots)$ where b is now the unknown function which we have

expanded as a power series in g . This leads to the following modified problem in terms of b :

$$\begin{aligned} v_b \frac{\partial b}{\partial \xi} &= v_p \frac{\partial b}{\partial \ell} + P(\xi) B_a(\xi + \ell) \\ &+ g \int_0^\xi b(y, \xi - y + \ell) P(\xi - y) dy \\ &+ g P(\ell) \int_\ell^\infty b(\xi, \ell') d\ell' \\ &- g b(\xi, \ell) \int_0^\ell P(\ell') d\ell'. \end{aligned}$$

What has been accomplished by the above assumption is that g no longer appears in the source term, and we can treat this as a perturbation problem for small g . The lowest order equation is:

$$v_b \frac{\partial b_0}{\partial \xi} - v_p \frac{\partial b_0}{\partial \ell} = P(\xi) B_a(\xi + \ell).$$

We introduce the natural coordinates,

$$w = v_p \xi + v_b \ell, \quad \zeta = v_b \xi - v_p \ell.$$

Then

$$\frac{\partial b_0}{\partial \zeta} = \mu P[\mu(v_p w + v_b \zeta)] B_a(v_s w + v_d \zeta),$$

where

$$\mu = 1/(v_b^2 + v_p^2), \quad v_s = \mu(v_b + v_p), \quad v_d = \mu(v_b - v_p).$$

To solve this to lowest order, we integrate

$$b(\zeta, w) = Q(w) + \int_0^\zeta \mu P[\mu(v_p w + v_b \zeta')] B_a(v_s w + v_d \zeta') d\zeta' \equiv Q(w) + R(w, \zeta).$$

Thus, to lowest order:

$$b_0(\xi, \ell) = Q(v_p \xi + v_b \ell) + R(v_p \xi + v_b \ell, v_b \xi - v_p \ell).$$

The boundary condition $b(0, \ell) = 0$ implies

$$0 = Q(v_b \ell) + R(v_b \ell, -v_p \ell),$$

or, letting $u = v_b \ell$,

$$Q(u) = -R(u, -(v_p/v_b)\zeta)$$

so that the complete solution is:

$$b_0(\xi, \ell) = -R(v_p \xi + v_b \ell, -\frac{v_p}{v_b} \xi - v_p \ell) + R(v_p \xi + v_b \ell, v_b \xi - v_p \ell).$$

With this, we could then move on to the next order term which has to satisfy the equation:

$$v_b \frac{\partial b_1}{\partial \xi} - v_p \frac{\partial b_1}{\partial \ell} = \int_0^\xi b_0(y, \xi - y + \ell) P(\xi - y) dy + P(\ell) \int_\ell^\infty b_0(\xi, \ell') d\ell' - b_0(\xi, \ell) \int_0^\ell P(\ell') d\ell'.$$

This can be solved in the same way as the previous order equation and the boundary condition $b_1(0, \ell) = 0$ yields a unique solution. We illustrate this in more detail using specific assumptions about the cutting probability below.

4.2.1. *Example: Cutting equally probable everywhere*

We now consider a very simple example which is nevertheless appealing. We will assume that for the capped filaments, the rate of severing is independent of the position, $P(\ell) = 1$. (It is reasonable to assume that most of these filaments are already in the ADP-actin form, so that the cutting probability is not strongly position-dependent.)

We also assume that $v_b = v_p$. This case is called the **treadmilling** case (Edelstein-Keshet and Ermentrout, 2000). By rescaling space, time, and length, we can assume $v_b = 1$ for simplicity. The lowest order equation is then:

$$b_0(\zeta, w) = Q(w) + \frac{1}{2} \int_0^\zeta B_a(w) d\zeta' = Q(w) + \frac{1}{2} B_a(w)\zeta.$$

Applying the definitions, $w = \xi + \ell$, $\zeta = \xi - \ell$ and the boundary condition, we get:

$$b_0(\xi, \ell) = \xi B_a(\xi + \ell).$$

Recalling that $B_a(\ell) = K_1 \ell \exp(-K_2 \ell^2)$ we see that

$$b_0(\xi, \ell) = K_1 \xi (\xi + \ell) e^{-K_2 (\xi + \ell)^2}.$$

We can get the length distribution by integrating this:

$$b_{0,length}(\ell) = \int_0^\infty b_0(\xi, \ell) d\xi = \frac{K_1 \sqrt{\pi}}{4K_2^{3/2}} \operatorname{erfc}(\sqrt{K_2} \ell)$$

where erfc is the complementary error function. Thus, to first order approximation, the tip distribution is:

$$b_{0,tip}(\xi) = \frac{K_1 \xi}{2K_2} e^{-K_2 \xi^2}.$$

This distribution has a peak at $\xi = 1/\sqrt{2K_2}$.

We can find the next order approximation, which takes the cutting into account. Without loss of generality, set $K_1 = 1$ since this is just a scale in a linear problem. We have to solve:

$$\frac{\partial b_1}{\partial \xi} - \frac{\partial b_1}{\partial \ell} = \frac{\xi}{2K_2} e^{-K_2(\xi+\ell)^2} (k_2 \xi^2 - K_2 \xi \ell + 1 - 2K_2 \ell^2)$$

with the boundary conditions. This again is quite easy to integrate since, after transforming to natural coordinates, the exponential term is independent of ζ . We then use MAPLE to do the algebra and obtain:

$$b_1(\xi, \ell) = \frac{\xi^2}{4K_2} e^{-K_2(\xi+\ell)^2} (1 - 2K_2 \xi \ell - 2K_2 \ell^2).$$

Note that this is negative for ξ, ℓ large enough so that the effect of fragmentation is to diminish the distribution for long lengths or far from the edge. An interesting point is that the integral of b_1 with respect to ℓ is identically 0 so that the cutting has only a higher order effect on the distribution of tips. However, the integral with respect to ξ is not 0 and so there is an effect on the length distribution.

Summarizing, to the first two orders, we have:

$$b(\xi, \ell) \approx e^{-K_2(\xi+\ell)^2} \left[\xi^2 + \ell \xi + \frac{g \xi^2}{4K_2} (1 - 2K_2 \xi \ell - 2K_2 \ell^2) \right]. \tag{11}$$

This expression has some interesting properties that are intuitively appealing. Consider the distribution of tips with short lengths. The effect of the choppers (g) is to produce more tips throughout the whole lamellipod since $v(\xi, \ell) \equiv (1 - 2K_2 \xi \ell - 2K_2 \ell^2)$ is positive for $\xi < (1 - 2K_2 \ell^2)/(2K_2 \ell)$. However, if ℓ is larger, then this expression is negative for smaller values of ξ and the result is that the tip number is diminished for distances away from the edge.

In Figures 7, 8, 9, 10 we show the structure of this solution for capped filament densities. The first of these figures shows the function $b(\xi, \ell)$ plotted versus both its arguments. (The label x represents ξ in the figure). The details of the distribution of the capped tips of these filaments, for various lengths is shown in Figure 8. To check how good this approximation is, we compare it to a numerical simulation of equation (10) in the next section. The results of this comparison are then shown in Figures 9 and 10.

4.2.2. Capped filament simulations

We must solve the following partial differential-integral equation:

$$\begin{aligned} v_b \frac{\partial B}{\partial \xi} &= v_p \frac{\partial B}{\partial \ell} + g S(\xi, \ell) \\ &+ g \int_0^\xi B(y, \xi - y + \ell) P(\xi - y) dy \\ &+ g P(\ell) \int_\ell^\infty B(\xi, \ell') d\ell' \\ &- g B(\xi, \ell) \int_0^\ell P(\ell') d\ell'. \end{aligned} \tag{12}$$

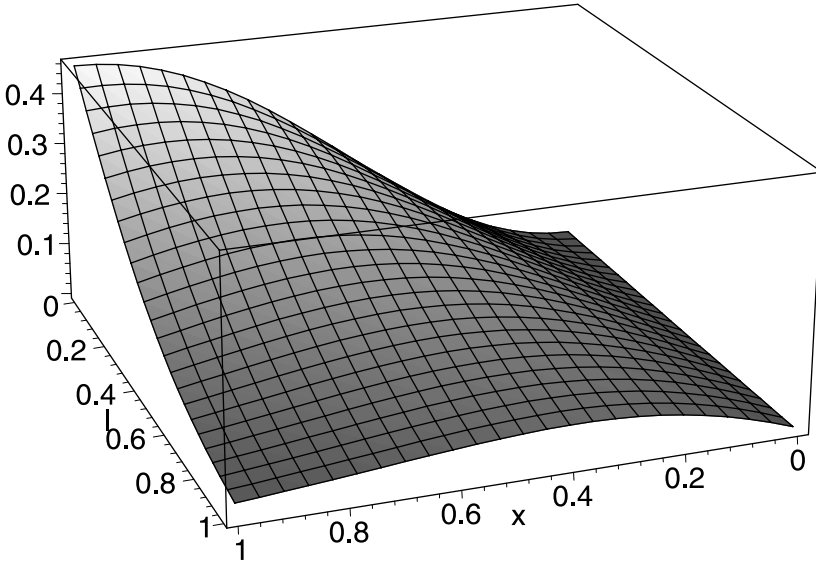


Fig. 7. The distribution of capped filaments over space and length. This is a plot generated by MAPLE of the function $b(x, l)$ given in equation (11), for $g = 1$ and $K_2 = 1$. This graph shows that most of the capped filaments are relatively short and located at some distance from the membrane (i.e. $x > 0$). The distribution of tips of these filaments and the length distribution are then shown in figures 8 and 9.

for the capped filament density with the boundary condition, $B(0, \ell) = 0$ and

$$S(\xi, \ell) = P(\xi)B_a(\xi + \ell)$$

as the source term. The form of this equation is fortuitous since in order to obtain $B(\xi_0, \ell)$ we need $B(\xi, \ell)$ for $\xi < \xi_0$. The same cannot be said for the variable ℓ . Thus, we can treat this as an *evolution* equation in the variable ξ . That is, given the data, $B(0, \ell) = 0$ we can just solve the Volterra integro-differential equation by integrating forward with respect to ξ . Thus, we discretize in the length ℓ , and solve a coupled set of (discretized) Volterra integro-differential equations using XPP with Euler’s method and a step size of 0.1. Smaller step sizes show no difference in the solutions. We have rescaled the variables ξ and ℓ by the constants v_b and v_p . To recover the unscaled variables, multiply the axes of Figure 10 by v_b and v_p .

Figure 9 shows three comparisons between the results of the numerical simulation of the above partial differential-integral equation, and of the asymptotic formula shown in equation (11). The distribution of the positions of the (capped) ends of the filaments are shown for lengths $\ell = 0, 1.5, 3.0$ for both simulation and asymptotic solution. It is apparent that the agreement is reasonably good. We note that longer filaments have their tips nearer to the leading edge than do the short lengths, i.e. the peak in the tip distribution is closer to $x = 0$ for the longer filaments, as observed previously.

Figure 10 shows the complete (ξ, ℓ) distribution for the approximate and the numerical solution. Here we show the distribution as a pair of density contour

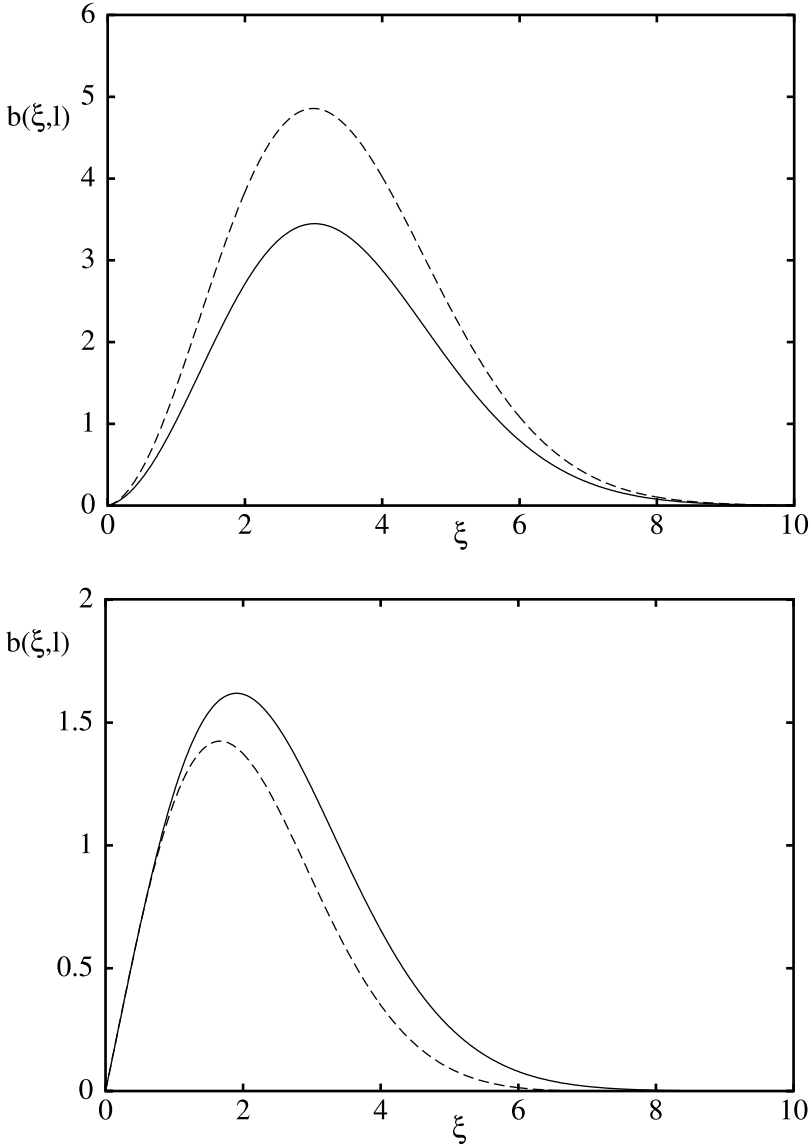


Fig. 8. The tip distribution for a fixed length of **capped** barbed end filaments for (A) small lengths (B) longer lengths. The two plots in each graph represent the effect of fragmentation. The dashed lines correspond to $g = 0.2$ and the solid lines to $g = 0.0$.

plots, rather than the 3D version of Figure 7. We could do similar simulations with more realistic cutting probabilities. However, on the analytic side, the resulting approximation leads to integrals that have no closed forms.

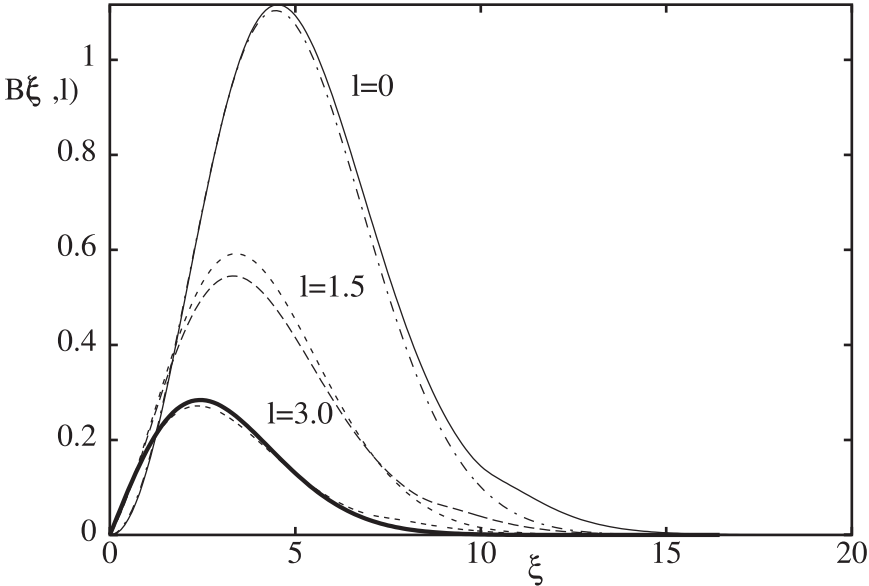


Fig. 9. Densities, B as a function of distance relative to the cell edge, ξ , for various lengths. Numerical and asymptotic solutions are shown for $l = 0, 1.5, 3.0$.

5. Comparison with experimental observations

Recent quantitative data for actin filament density distributions appear in a number of papers in the literature, mostly as scans of fluorescently labeled actin across the lamellipod (Redmond and Zigmond, 1993; Baily et al., 1999; Small et al., 1995b; Svitkina and Borisy, 1999). Svitkina and Borisy (1999) studied the distribution of actin associated proteins such as Arp2/3, and ADF/cofilin in the lamellipodia of *Xenopus laevis* keratocytes and fibroblasts. In so doing, they also characterized (for comparison and relative placement) the actin density by phalloidin staining. Shown in their Figures 5 a', b', c', and Figure 8 d (red curves) are actin distributions. In this section, we use the results from Figure 8d of their paper to compare to our predicted actin filament density. As in our model, the above authors find a graded actin filament length distribution, and a peak of barbed ends close to the membrane. Pointed ends appear to be distributed across the lamellipod, and loss of actin filaments in the rear portions appeared connected largely to depolymerization of the pointed ends.

In analyzing our model, in Section 5, we made the simplifying assumption that all uncapped barbed ends were concentrated right at the cell edge, i.e. we assumed a delta-function distribution of their spatial location. This simplification allowed us to find explicit solutions of an otherwise intractable problem. In reality, the uncapped filament ends are spatially distributed in some narrow zone close to the cell edge, and this finite width is essential for comparison with the experimental results. (Note: if all uncapped barbed ends are at $x = 0$ then the actin density close to the

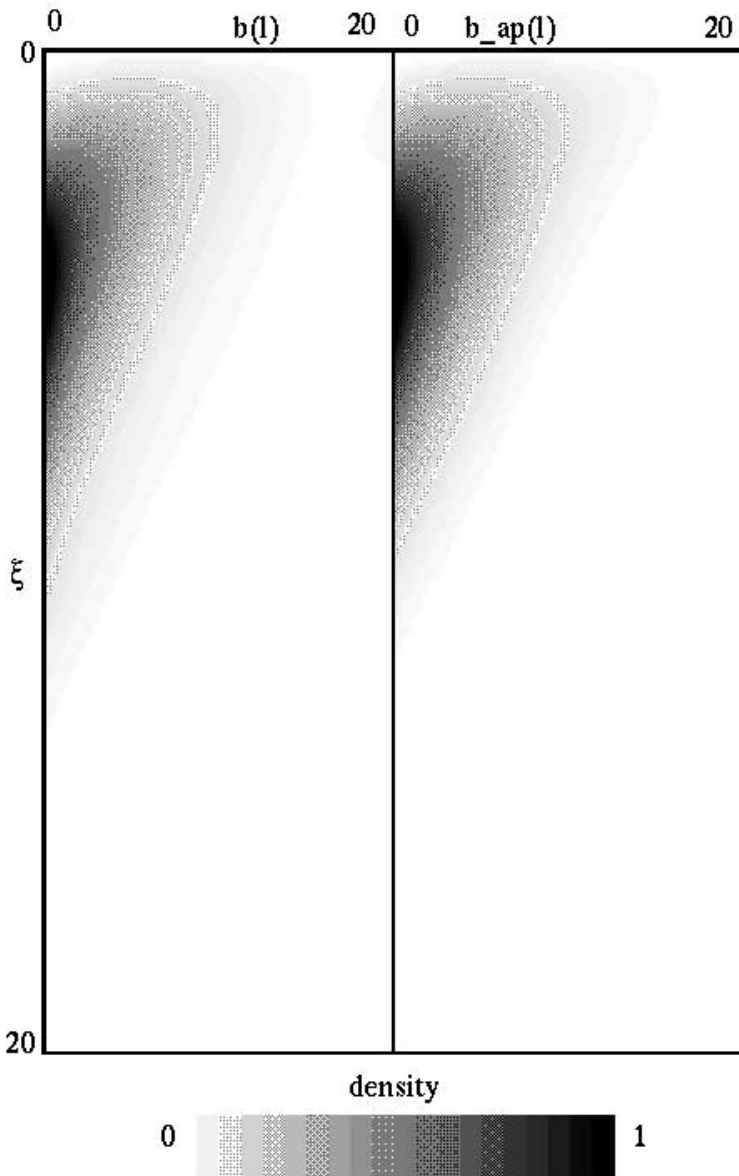


Fig. 10. Densities of $B(\xi, l)$ comparing the numerical solution to equation (12) – left distribution shown – with the approximate solution given by the formula (11) for the simple case of equally probable cutting - right distribution. Scales are identical in both cases. The vertical axis is the moving variable ξ and the horizontal is the length, l . The darker areas represent higher densities.

edge would be a monotonic decreasing function, unlike the sharp but finite rise in density seen experimentally in the scans described above.)

For purposes of comparison, we dropped the assumption that tips are located exactly at the membrane. Thus, we solve the steady state equation (12) but use a more general function $\Lambda(\xi)$ rather than the delta function assumed in section 4. Because we are treating the steady state problem, (as described in the previous section) certain integrals must be computed symbolically and then used as inputs to the capped filament equations. This limits the variety of choices for functions such as $\Lambda(\xi)$ that we can handle with the current simulation technique, but nevertheless produces interesting preliminary results. For these runs, we assumed that $\Lambda(\xi)$ is constant for some interval between $0 < \xi < \xi_0$, i.e that active barbed ends are distributed uniformly within a narrow strip of width ξ_0 close to the membrane.

In order to compare model results to experimental results, it is necessary to calculate the the stationary distribution of the *total actin density* due to both capped and uncapped filaments, as a function of distance from the cell edge, i.e we also computed the total filamentous actin density:

$$Z(\xi) = \int_0^\xi \int_{\xi-s}^\infty b_a(s, \ell) + b_c(s, \ell) d\ell ds$$

as a function of position relative to the moving edge. We computed this given b_c and the formula for b_a . The quantity Z is “computed on the fly” by solving the associated evolution equation for $Z(\xi)$:

$$\frac{dZ}{d\xi} = \int_0^\infty B_T(\xi, \ell) d\ell - \int_0^\xi B_T(s, \xi - s) ds$$

where $B_T = b_a + b_c$. The set of equations are numerically integrated using XPP, freely available software: (<http://www.math.pitt.edu/~bard/xpp/xpp.html>). For this initial numerical exploration, we took the fragmentation probability, $P(l)$, to be constant. By previous results, we assumed that filaments with uncapped barbed ends had a steady-state length distribution of the form

$$b_a(\ell) = k_1 \ell \exp(-k_2 \ell^2).$$

We use $b_c(0, \ell) = 0$ for initial data as there are no capped filaments at the edge.

Figure 11 shows how the actin filament density varies over space from the edge of the cell into the body of the lamellipod. (The origin is at the moving cell edge, and the horizontal axis is oriented into the cell, measuring distance from the edge.) A comparison is shown of various profiles that differ only in the magnitude of the fragmentation rate. If the parameter g is low, i.e there is little fragmentation, then the peak occurs close to the point at which the active barbed end zone ends, ξ_0 . As g increases, the peak shifts further back from the membrane, into the cell interior. Moreover, the density at the back of the lamellipod actually increases as g increases. This result is somewhat counterintuitive. However, it can be understood as follows: with no fragmentation at all, the model would predict that barbed end filaments “treadmill” along, preserving their stationary length distribution- and also

Actin

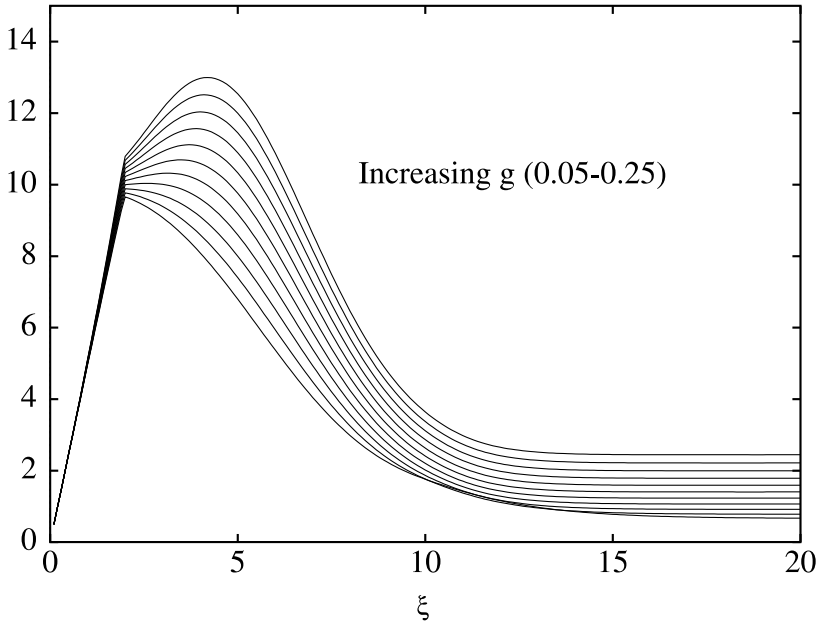


Fig. 11. A plot of the stationary distribution of total actin filament density as a function of distance predicted by the model. We used a uniform distribution of active barbed ends over the region, $0 < x < 2$ and set $k_2 = .05$. The curves represent a variety of values of the fragmentation rate, g . (Topmost curve has highest rate of actin filament fragmentation.)

fully determining the filament density throughout the structure. According to previous discussion, this would mean that the density of polymerized actin is seen to drop off beyond some distance away from the edge. As fragmentation is turned on, the tails of some of these filaments get “left behind”: These tails have capped barbed ends, so they cannot keep up with the front-runner actin filaments. The chopped tails thus contribute to increasing the density in the back. (i.e. their density appears to move rearwards relative to the coordinate system moving with the cell edge).

Figure 12 shows a typical numerical solution of the model (solid curve) superimposed directly on experimental data extracted from Figure 8d in the paper by Svitkina and Borisy (1999). (Scans shown in the online version of their paper were converted to bitmaps, and a C program was written to extract (x, y) coordinates of the nonzero entries. These were then scaled and plotted on the same figure as our numerical results.) We varied the main free parameters, k_2 , g and ξ_0 . (Other free parameters are the overall length scale and the magnitude.) The parameter k_1 scales the magnitude of the source and was used to fit the amplitude. The parameter r scales the length. We scaled the length of the lamellipod and the amplitude to fit the overall dimensions (e.g. peak magnitude) of the data. The parameter ξ_0 affects the position of the peak relative to the initial linear rise of the actin concentration. ξ_0 , g and k_2 affect the decay rate. These required finer tuning. For the figures we

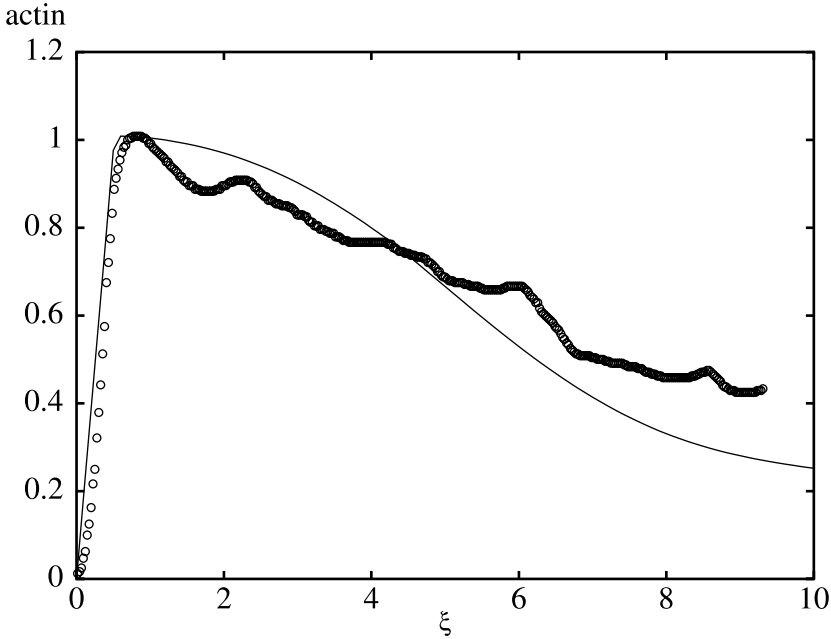


Fig. 12. A comparison between model predictions and experimentally observed actin densities. Shown is actin filament density over a lamellipod length of 10 units with the active density uniform over the interval $[0, 0.56]$. The parameters values are $k_2 = 0.04$ and $g = 0.1$. The solid curve represents simulation results, and is superimposed over experimental data for actin filament density from (Svitkina and Borisy, 1999). Parameters were fitted visually.

set $k_2 = 0.05$, $\xi_0 = 0.55$, $r = 0.1$, $g = 0.05$. The agreement is reasonable given that we have not attempted to capture many of the more subtle details of the actin dynamics.

6. Discussion

The comparison of theoretical and experimental results shown in Figure 12 reveals that an overall similarity in actin filament density is not difficult to produce by visual fitting of the parameters. This qualitative agreement is not surprising, and, indeed, would make it difficult to make fine distinctions between alternate hypotheses for the way that fragmentation and/or depolymerization occurs. Nevertheless, the comparison also demonstrates that there may be non-stationary processes, such as periodic “flares” of barbed end nucleation that lead to the waves in density seen in the real distribution that our model does not reflect.

Our results should be interpreted with a healthy dose of skepticism, as they are based on a rather naive set of assumptions for the way that the cytoskeleton is behaving. The purpose here was to show how one could take into account both length and spatial distribution of filaments, whereas in previous models only dependence on one or the other variable was modelled.

Future work might be directed at incorporating several important factors that have been omitted in this paper: (1) The mechanics of membrane motion, and how actin polymerization is related to protrusion (2) The nucleation of new barbed ends close to the edge of the cell by the recently discovered complex Arp2/3, (3) A greater level of detail about the way that filaments disintegrate at their older parts (4) More detail about monomer recycling and sequestration by thymosin and profilin. Many of these factors have already been considered in a quantitative model for rapid cell motion (Mogilner and Edelstein-Keshet, 2001), where neither the detailed actin density distribution, nor the filament length distribution was of primary concern. Non-stationary (transient) effects, such as response to chemoattractants, and the resulting changes in the cytoskeleton would also be of interest.

The study of the cytoskeleton, and actin in particular, has been advancing in great steps in the biological literature, and the influence of numerous details, including signal transduction events is now beginning to be understood. Possibly, models such as the present one will have some role to play in the understanding of the actin polymerization as a whole. While the details come into clearer focus through experimentation, we can only hope to try to understand some of the basic interactions, at a rather incomplete level of detail.

Acknowledgements. The authors would like to thank Alex Mogilner for insightful advice and comments. LEK is supported under an Operating Grant from NSERC (Canada). GBE is supported by NSF grant DMS 9972913.

References

- Arora, P.D., McCulloch, C.A.G.: Dependence of fibroblast migration on actin severing activity of gelsolin, *J Biol Chem.*, **271**(34), 20516–23 (1996)
- Arber, S., Barbayannis, F.A., Hanser, H., Schneider, C., Stanyon, C.A., Bernard, O., Caroni, P.: Regulation of actin dynamics through phosphorylation of cofilin by LIM-kinase, *Nature*, **393**, 805–808 (1998)
- Alberts, B., Bray, D., Lewis, J., Raff, M., Roberts, K., Watson, J.D.: *Molecular Biology of the Cell*, *Garland*, New York (1989)
- Bailly, M., Macaluso, F., Cammer, M., Chan, A., Segall, J.E., Condeelis, J.S.: Relationship between Arp2/3 complex and the barbed ends of actin filaments at the leading edge of carcinoma cells after epidermal growth factor stimulation, *J Cell Biol.*, **145**(2), 331–345 (1999)
- Brenner, S.L., Korn, E.D.: On the mechanism of actin monomer-polymer subunit exchange at steady state, *J Biol Chem.*, **258**, 5013–5020 (1983)
- Blanchoin, L., Pollard, T.D.: Mechanism of Interaction of Acanthamoeba Actophorin (ADF/Cofilin) with Actin Filaments, *J Biol Chem.*, **247**(22), 15538–15546 (1999)
- Cano, M.L., Cassimeris, L., Fechheimer, M., Zigmond, S.H.: Mechanisms responsible for F-actin stabilization after lysis of Polymorphonuclear Leukocytes, *J. Cell Biol.*, **116**(5), 1123–1134 (1992)
- Cano, M.L., Lauffenburger, D.A., Zigmond, S.H.: Kinetic analysis of F-actin depolymerization in Polymorphonuclear Leukocyte lysates indicates that chemoattractant stimulation increases actin filament number without altering the filament length distribution, *J. Cell. Biol.*, **115**(3), 677–687 (1991)

- Carlier, M., Laurent, V., Santolini, J., Melki, R., Didry, D., Xia, G., Hong, Y., Chua, N., Pantaloni, D.: Actin Depolymerizing Factor (ADF/Cofilin) enhances the rate of filament turnover: implications in actin-based motility, *J. Cell Biol.*, **136**(6), 1307–1323 (1997)
- Carlier, M., Pantaloni, D.: Control of Actin dynamics in cell motility, *J. Mol. Biol.*, **269**, 459–467 (1997)
- Cassimeris, L., McNeill, H., Zygmund, S.H.: Chemoattractant-stimulated Polymorphonuclear Leukocytes contain two populations of actin filaments that differ in their spatial distributions and relative stabilities, *J. Cell Biol.*, **110**, 1067–1075 (1990)
- Coluccio, L.M., Tilney, L.G.: Under physiological conditions actin disassembles slowly from the nonpreferred end of an actin filament, *J. Cell Biol.*, **97**, 1629–1634 (1983)
- Cunningham, C.C., Stossel, T.P., Kwiatkowski, D.J.: Enhanced motility in NIH 3T3 fibroblasts that overexpress gelsolin, *Science*, **251**(4998), 1233–6 (1991)
- Civelekoglu, G., Edelstein-Keshet, L.: Models for the formation of actin structures, *Bull Math Biol.*, **56**, 587–616 (1994)
- Dufort, P.: *Computational modelling of nucleotide processing by the actin cytoskeleton regulatory network*, PhD thesis, U Toronto, (2000)
- Dufort, P.A., Lumsden, C.J.: How Profilin/Barbed-end synergy controls actin polymerization: a kinetic model of the ATP hydrolysis circuit, *Cell Motil. Cytoskel.*, **35**, 309–330 (1996)
- DiNubile, M.J., Huang, S.: High concentrations of phosphatidylinositol-4-5-bisphosphate may promote actin filament growth by three potential mechanisms: inhibiting capping by neutrophil lysates, severing actin filaments, and removing capping protein- β_2 from barbed ends, *Biochim. Biophys. Acta.*, **1358**, 261–278 (1997)
- Edelstein-Keshet, L., Ermentrout, G.B.: Models for the length distribution of actin filaments I: Simple polymerization and fragmentation, *Bull Math Biol.*, **60**(3), 449–475 (1998)
- Edelstein-Keshet, L., Ermentrout, G.B.: Models for spatial polymerization dynamics of rod-like polymers, *J Math Biol.*, **40**(1), 64–96 (2000)
- Ermentrout, G.B., Edelstein-Keshet, L.: Models for the length distribution of actin filaments II: Polymerization and fragmentation by gelsolin acting together, *Bull Math Biol.*, **60**(3), 477–503 (1998)
- Edelstein-Keshet, L.: Mathematical approaches to cytoskeletal assembly, *European Biophysics Journal.*, **27**, 521–531 (1998)
- Heath, J., Holifield, B.: News and Views: Actin alone in lamellipodia, *Nature*, **352**, 107–108 (1991)
- Howard, T., Chaponnier, C., Yin, H., Stossel, T.: Gelsolin-actin interaction and actin polymerization in human neutrophils, *J Cell Biol.*, **110**, 1983–1991 (1990)
- Isenberg, G., Niggli, V.: Interaction of cytoskeletal proteins with membrane lipids, *Int. Rev. Cytol.*, **178**, 73–125 (1998)
- Janmey, P.A.: Phosphoinositides and calcium as regulators of cellular actin assembly and disassembly, *Annu. Rev. Physiol.*, **56**, 169–191 (1994)
- Korn, E.D., Carlier, M., Pantaloni, D.: Actin filament polymerization and ATP hydrolysis, *Science*, **238**, 638–644 (1987)
- Lind, S.E., Janmey, P.A., Chaponnier, C., Herbert, T.J., Stossel, T.P.: Reversible binding of actin to gelsolin and profilin in human platelet extracts, *J Cell Biol.*, **105**, 883–842 (1987)
- Meberg, P.J., Ono, S., Minamide, L.S., Takahashi, M., Bamburg, J.R.: Actin depolymerizing factor and cofilin phosphorylation dynamics: response to signals that regulate neurite extension, *Cell Motil. Cytoskel.*, **39**, 172–190 (1998)
- Mogilner, A., Edelstein-Keshet, L.: Rapid Cell Motion is based on robust, spatial regulation of actin dynamics: A quantitative analysis, *Manuscript.*, (2001)
- Moon, A., Drubin, D.G.: The ADF/Cofilin proteins: stimulus-responsive modulators of actin dynamics, *Molec. Biol. Cell.*, **6**, 1423–1431 (1995)

- Mogilner, A., Edelstein-Keshet, L.: Selecting a common direction I. How orientational order can arise from simple contact responses between interacting cells, *J Math Biol.*, **33**, 619–660 (1995)
- Mogilner, A., Edelstein-Keshet, L.: Spatio-angular order in populations of self-aligning objects: formation of oriented patches, *Physica D.*, **89**, 346–367 (1996)
- Mullins, R.D., Heuser, J.A., Pollard, T.D.: The interaction of Arp2/3 complex with actin: Nucleation, high affinity pointed end capping, and formation of branching networks of filaments, *PNAS*, **95**(11), 6181–6186 (1998)
- McGough, A., Way, M.: Molecular model of an actin filament capped by a severing protein, *J. Struct. Biol.*, **15**, 144–150 (1995)
- Mogilner, A., Oster, G.: The physics of lamellipodial protrusion, *Eur Biophys J.*, **25**, 47–53 (1996)
- Mogilner, A., Oster, G.: Cell motility driven by actin polymerization, *Biophys. J.*, **71**, 3030–3045 (1996)
- Marchand, J-B., Moreau, P., Paoletti, A., Cossart, P., Carlier, M-F., Pantaloni, D.: Actin-based movement of *Listeria monocytogenes*: actin assembly results from the local maintenance of uncapped filament barbed ends at the bacterium surface, *J. Cell. Biol.*, **130**, 331–343 (1995)
- Oster, G.F.: Biophysics of Cell Motility, Lecture Notes, University of California Berkeley (1994)
- Oster, G.F.: On the crawling of cells, *J. Embryol exp Morph Suppl*, **83**, 329–364 (1984)
- Pollard, T.D.: Rate constants for the reactions of ATP- and ADP- actin with the ends of actin filaments, *J Cell Biol.*, **103** (6 pt 2), 2747–2754 (1986)
- Mullins, R.D., Heuser, J.A., Pollard, T.D.: The interaction of Arp2/3 complex with actin: Nucleation, high affinity pointed end capping, and formation of branching networks of filaments, *PNAS*, **95**(11), 6181–6186 (1998)
- Redmond, T., Zigmond, S.H.: Distribution of F-Actin elongation sites in lysed Polymorphonuclear Leukocytes parallels the distribution of endogenous F-actin, *Cell Motil. Cytoskel.*, **26**, 1–18 (1993)
- Ryder, M.I., Weinreb, R.N., Niederman, R.: The organization of actin filaments in human polymorphonuclear leukocytes, *Anat. Rec.*, **209**, 7–20 (1984)
- Rehder, V., Cheng, S.: Autonomous regulation of growth cone filopodia, *J. Neurobiol.*, **34**(2), 179–192 (1998)
- Rosenblatt, J., Mitchison, T.J.: Actin, cofilin and cognition, *Nature*, **393**, 739–740 (1998)
- Tilney, L.G., Bonder, E.M., DeRosier, D.J.: Actin filaments elongate from their membrane associated ends, *J. Cell. Biol.*, **90**, 485–494 (1981)
- Tilney, L.G., Jaffe, L.A.: Actin, microvilli, and the fertilization cone of sea urchin eggs, *J. Cell Biology.*, **87**, 771–782 (1980)
- Schafer, D.A., Jennings, P.B., Cooper, J.A.: Dynamics of capping protein and actin assembly in vitro: uncapping barbed ends by polyphosphoinositides, *J. Cell Biol.*, **135**, 169–179 (1996)
- Small, J.V., Isenberg, G., Celis, J.E.: Polarity of actin at the leading edge of cultured cells, *Nature*, **272**, 638–639 (1978)
- Small, J.V., Herzog, M., Anderson, K.: Actin filament organization in the fish keratocyte lamellipodium, *J Cell Biol.*, **129**(5), 1275–1286 (1995a)
- Small, J.V., Monika, H., Kurt, A.: Actin filament organization in the fish keratocyte lamellipodium, *J Cell Biology.*, **129**(5), 1275–1286 (1995b)
- Svitkina, T.M., Borisy, G.G.: Arp2/3 complex and actin depolymerizing factor/cofilin in dendritic organization and treadmilling of actin filament array in lamellipodia, *J. Cell Biol.*, **145**(5), 1009–1026 (1999)

- Spiros, A., Edelstein-Keshet, L.: Testing a model for the dynamics of actin structures with biological parameter values, *Bull. Math. Biol.*, **60**(2), 275–305 (1998)
- Theriot, J.A.: Actin filament dynamics in cell motility, *Actin: Biophysics, Biochemistry, and Cell Biology.*, J.E. Estes and P.J. Higgins, 133–145, Plenum Press, New York (1994)
- Theriot, J.A., Mitchison, T.J.: Actin microfilament dynamics in locomoting cells, *Nature*, **352**, 126–131 (1991)
- Witke, W., Sharpe, A.H., Hartwig, J.H., Azuma, T., Stossel, T.P., Kwiatkowski, D.J.: Hemostatic, inflammatory, and fibroblast responses are blunted in mice lacking gelsolin, *Cell.*, **81**, 41–51 (1995)
- Wang, Y.-L.: Exchange of actin subunits at the leading edge of living fibroblasts: possible role of treadmilling, *J. Cell Biol.*, **101**, 597–602 (1985)
- Welch, M.D., Mallavarapu, A., Rosenblatt, J., Mitchison, T.J.: Actin dynamics *in vivo*, *Curr Op Cell Bio.*, **9**, 54–61 (1997)
- Yang, N., Higuchi, O., Ohashi, K., Nagata, K., Wada, A., Kangawa, K., Nishida, E., Mizuno, K.: Cofilin phosphorylation by LIM-kinase 1 and its role in Rac-mediated actin reorganization, *Nature*, **393**, 809–812 (1998)
- Zigmond, S.H.: Recent quantitative studies of actin filament turnover during cell locomotion, *Cell Motil. Cytoskel.*, **25**, 309–316 (1993)
- Zigmond, S.H., Joyce, M., Yang, C., Brown, K., Huang, M., Pring, M.: Mechanism of Cdc42-induced actin polymerization in neutrophil extracts, *J. Cell Biol.*, **142**(4), 1001–1012 (1998)